CHALMERS
FINITE ELEMENT CENTER

PREPRINT 2001-02

The $\mathcal{LL}^*$ Finite Element Method and Multigrid for the Magnetostatic Problem

Rickard Bergström, Mats G. Larson, and Klas Samuelsson

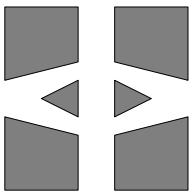

Chalmers Finite Element Center
CHALMERS UNIVERSITY OF TECHNOLOGY
Göteborg Sweden 2001

CHALMERS FINITE ELEMENT CENTER

Preprint 2001-02

The $\mathcal{LL}^*$ Finite Element Method and Multigrid for the Magnetostatic Problem

Rickard Bergström, Mats G. Larson, and Klas Samuelsson

CHALMERS

Chalmers Finite Element Center
Chalmers University of Technology
SE–412 96 Göteborg Sweden
Göteborg, March 2001

The $\mathcal{LL}^*$ Finite Element Method and Multigrid for the Magnetostatic Problem
Rickard Bergström, Mats G. Larson, and Klas Samuelsson
NO 2001-02
ISSN 1404–4382

Chalmers Finite Element Center
Chalmers University of Technology
SE–412 96 Göteborg
Sweden
Telephone: +46 (0)31 772 1000
Fax: +46 (0)31 772 3595
`www.phi.chalmers.se`

Printed in Sweden
Chalmers University of Technology
Göteborg, Sweden 2001

THE $\mathcal{LL}^*$ FINITE ELEMENT METHOD AND MULTIGRID FOR THE MAGNETOSTATIC PROBLEM

RICKARD BERGSTRÖM, MATS G. LARSON, AND KLAS SAMUELSSON

ABSTRACT. We develop the $\mathcal{LL}^*$ method for a magnetostatic model problem in electromagnetics with large jumps in material parameters in three spatial dimensions. A priori and a posteriori error estimates are presented as well as an adaptive algorithm. We employ a multigrid method to solve the resulting algebraic equations. Finally, we present numerical results.

1. INTRODUCTION

In this paper we are concerned with finite element approximation of first order elliptic partial differential equations of the form $\mathcal{L}u = f$. More precisely, we study a model problem from magnetostatics in three spatial dimensions with large jumps in the material coefficients. Typically, due to corners in the geometry, the solution develops singularities and does not reside in H^1, and thus cannot be accurately approximated in spaces of continuous piecewise polynomials. As a remedy we instead introduce the dual variable v such that $u = \mathcal{M}\mathcal{L}^*v$, where $\mathcal{M}$ is a bounded symmetric operator with bounded inverse. Substituting into the equation $\mathcal{L}u = f$ we obtain the symmetric second order problem $\mathcal{L}\mathcal{M}\mathcal{L}^*v = f$, which can be approximated by standard continuous polynomials, since $v \in H^1$. Choosing $\mathcal{M}$ properly, the energy minimized is the physical energy, which is a desireable property. We refer to this approach as the $\mathcal{LL}^*$-method. The resulting algebraic system is symmetric positive definite and can be efficiently solved by a multigrid method.

The $\mathcal{LL}^*$-method was recently suggested by Cai et al [11] for solving a second order elliptic problem by first rewriting it as a first order system of equations and then applying the aforementioned approach. Here the method is viewed as a remedy of the difficulties which the Least Squares finite element method exhibits on problems which are not sufficiently regular. The least squares method, see for instance [3], [5], [6], [13], and the references therein, determines an approximate solution u_h which minimizes the L^2-norm of the residual $\|\mathcal{L}u_h - f\|^2$. Thus u is required to be in H^1 for the residual to be well defined. It is also shown that $\mathcal{LL}^*$-method is closely related to least squares methods based on weak norms of the residual, see Bramble et al [7] and Cai et al [10].

We may also view the $\mathcal{LL}^*$-method as a generalization of the classical potential methods in electromagnetics, see for instance Jin [15] for a general introduction to such techniques.

Date: March 1, 2001.

Chalmers Finite Element Center, Chalmers University of Technology, 412 96 Göteborg,
e-mail: {ribe, mgl, klassam}@ math.chalmers.se.

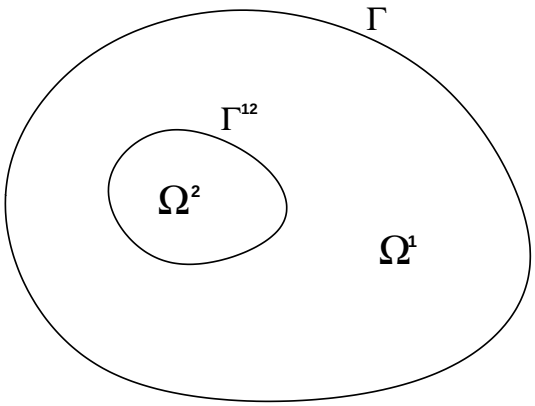

FIGURE 1. The notation used when a region is split into subregions.

In the case of the $\mathcal{LL}^*$-method, we allow for a more general potential v defined by $u = \mathcal{ML}^*v$.

We prove optimal a priori and a posteriori error estimates and based on the later we develop an adaptive algorithm for refinement of the mesh. We also discuss implementation details of the mesh refinement algorithm.

The remainder of the paper is organized as follows: in Section 2 we introduce the model problem and derive the $\mathcal{LL}^*$-method; in Section 3 we prove a priori and posteriori error estimates and describe the adaptive algorithm together with some details on the meshrefinement procedure; in Section 4 we formulate the multigrid algorithm; in Section 5 we present some numerical results.

2. The $\mathcal{LL}^*$ formulation

2.1. **A magnetostatic model problem.** Assume that $\Omega = \bigcup_{i=1}^{n} \Omega^i \in \mathbf{R}^3$, and denote the interface between regions Ω^i and Ω^j by Γ^{ij}, with $i < j$, see Figure 1. Assume that each subdomain have the magnetic permeability $\mu|_{\Omega^i} = \mu_r^i \, \mu_0$. The magnetostatic system then takes the form:

$$\nabla \times \mu^{-1} B = J \quad \text{in } \Omega^i, \tag{2.1a}$$

$$\nabla \cdot B = 0 \quad \text{in } \Omega^i, \tag{2.1b}$$

$$n \cdot B = 0 \quad \text{on } \Gamma, \tag{2.1c}$$

and the interface conditions

$$[\mu^{-1} B] \times n = 0 \quad \text{on } \Gamma^{ij}, \tag{2.2a}$$

$$[B] \cdot n = 0 \quad \text{on } \Gamma^{ij}. \tag{2.2b}$$

hold. Here, n is the exterior unit normal on the boundary Γ and a fixed unit normal on each interior interface Γ^{ij}, and $[u(x)] = \lim_{s \to 0^+} u(x + sn) - u(x - sn)$ with $x \in \Gamma^{ij}$, denotes the jump in u across the interface Γ^{ij}. Furthermore, it is easy to see that it is necessary

that

$$\nabla \cdot J = 0, \tag{2.3}$$

for (2.1) to have a solution.

2.2. **An associated first order operator.** By adding a slack variable b to (2.1) we can show ellipticity of this system [14]. This extra variable is in fact zero in the continuous problem as we show below, but this is not necessarily the case in the discrete problem. Furthermore, adding the slack variable creates a suitable Hilbert space setting for the analysis.

The extended system thus becomes

$$\nabla \times \mu^{-1} B - \nabla b = J \quad \text{in } \Omega, \tag{2.4a}$$

$$\nabla \cdot B = 0 \quad \text{in } \Omega, \tag{2.4b}$$

$$n \cdot B = 0 \quad \text{on } \Gamma, \tag{2.4c}$$

$$b = 0 \quad \text{on } \Gamma, \tag{2.4d}$$

$$[\mu^{-1} B] \times n = 0 \quad \text{on } \Gamma^{ij}, \tag{2.4e}$$

$$[B] \cdot n = 0 \quad \text{on } \Gamma^{ij}. \tag{2.4f}$$

The slack variable b is identically zero, since taking the divergence of (2.4a) we get the following Poisson problem for b:

$$-\Delta b = \nabla \cdot J - \nabla \cdot (\nabla \times \mu^{-1} B) \quad \text{in } \Omega, \tag{2.5}$$

together with the boundary condition (2.4d). From equations (2.1), (2.2) and (2.3) we see that the right hand side of (2.5) is zero, thus b is indeed zero and hence system (2.4) is equivalent to (2.1).

We introduce the Hilbert space

$$\mathcal{V} = [L^2(\Omega)]^3 \times L^2(\Omega), \tag{2.6}$$

and employ the notation $\boldsymbol{V} = [V\, v]^T \in \mathcal{V}$, with $V \in [L^2(\Omega)]^3$ and $v \in L^2(\Omega)$. Next we define the first order operator $\mathcal{L}$ and its formal adjoint $\mathcal{L}^*$ as follows

$$\mathcal{L}\boldsymbol{V} = \begin{pmatrix} \nabla \times \mu^{-1} V - \nabla v \\ \nabla \cdot V \end{pmatrix}, \quad \mathcal{L}^*\boldsymbol{W} = \begin{pmatrix} \mu^{-1} \nabla \times W - \nabla w \\ \nabla \cdot W \end{pmatrix}, \tag{2.7}$$

for $\boldsymbol{V}, \boldsymbol{W} \in \mathcal{V}$.

To derive the boundary conditions associated with $\mathcal{L}^*$ we compute

$$\begin{aligned} (\mathcal{L}\boldsymbol{V}, \boldsymbol{W}) &= (\boldsymbol{V}, \mathcal{L}^*\boldsymbol{W}) + \int_\Gamma n \times (\mu^{-1} V) \cdot W + \int_\Gamma v\; n \cdot W + \int_\Gamma n \cdot V\; w \\ &= (\boldsymbol{V}, \mathcal{L}^*\boldsymbol{W}) + \int_\Gamma n \times (\mu^{-1} V) \cdot W, \end{aligned} \tag{2.8}$$

where we used (2.4c) and (2.4d). Using the scalar triple product $n \times (\mu^{-1}V) \cdot W = -(\mu^{-1}V) \cdot n \times W$, and thus the remaining boundary term vanishes if and only if the condition

$$n \times W = 0 \quad \text{on } \Gamma, \tag{2.9}$$

holds.

The domains of $\mathcal{L}$ and $\mathcal{L}^*$ are,

$$\mathcal{D}(\mathcal{L}) = \{\boldsymbol{V} \in H(\nabla \times \mu^{-1}, \Omega) \cap H(\nabla\cdot, \Omega) \times H^1(\Omega) : n \cdot V = 0, v = 0\}, \tag{2.10a}$$

$$\mathcal{D}(\mathcal{L}^*) = \{\boldsymbol{V} \in H(\nabla\times, \Omega) \cap H(\nabla\cdot, \Omega) \times H^1(\Omega)/\,\mathbf{R} : n \times V = 0\}, \tag{2.10b}$$

where

$$H(\nabla \times \mu^{-1}, \Omega) = \{V \in [L^2(\Omega)]^3 : \nabla \times \mu^{-1}V \in [L^2(\Omega)]^3\}, \tag{2.11a}$$

$$H(\nabla\cdot, \Omega) = \{V \in [L^2(\Omega)]^3 : \nabla \cdot V \in L^2(\Omega)\}, \tag{2.11b}$$

are Hilbert spaces with the norms

$$\|V\|^2_{H(\nabla\times\mu^{-1},\Omega)} = \|V\|^2 + \|\nabla \times \mu^{-1}V\|^2, \tag{2.12a}$$

$$\|V\|^2_{H(\nabla\cdot,\Omega)} = \|V\|^2 + \|\nabla \cdot V\|^2. \tag{2.12b}$$

$H(\nabla\times, \Omega)$ corresponds to (2.11a) with $\mu = 1$. Thus, $\mathcal{D}(\mathcal{L})$ and $\mathcal{D}(\mathcal{L}^*)$ are Hilbert spaces, dense in $\mathcal{V}$, under the product norm

$$\|\boldsymbol{V}\|^2_{\mathcal{D}(\mathcal{L})} = \|V\|^2 + \|\nabla \times \mu^{-1}V\|^2 + \|\nabla \cdot V\|^2 + \|v\|^2_1, \tag{2.13}$$

and similarly for $\mathcal{D}(\mathcal{L}^*)$.

2.3. **The $\mathcal{L}\mathcal{L}^*$ variational formulation.** We can now in a standard manner derive a variational problem for (2.1) by integrating by parts: find $\boldsymbol{B} \in \mathcal{D}(\mathcal{L})$ such that

$$(\boldsymbol{J}, \boldsymbol{V}) = (\mathcal{L}\boldsymbol{B}, \boldsymbol{V}) = (\boldsymbol{B}, \mathcal{L}^*\boldsymbol{V}), \tag{2.14}$$

for all $\boldsymbol{V} \in \mathcal{D}(\mathcal{L}^*)$.

Next we introduce dual variables $\boldsymbol{U}$ such that

$$\boldsymbol{B} = \mathcal{M}\mathcal{L}^*\boldsymbol{U}, \tag{2.15}$$

where $\mathcal{M}$ denotes a symmetric positive definite bounded operator with bounded inverse. A suitable choice of $\mathcal{M}$ is presented below. Thus, we obtain the weak problem: find $\boldsymbol{U} \in \mathcal{D}(\mathcal{L}^*)$ such that

$$a(\boldsymbol{U}, \boldsymbol{V}) = l(\boldsymbol{V}), \tag{2.16}$$

for all $\boldsymbol{V} \in \mathcal{D}(\mathcal{L}^*)$. Here the bilinear form and functional are defined by

$$a(\boldsymbol{U}, \boldsymbol{V}) = (\mathcal{M}\mathcal{L}^*\boldsymbol{U}, \mathcal{L}^*\boldsymbol{V}), \tag{2.17}$$

$$l(\boldsymbol{V}) = (J, V). \tag{2.18}$$

We now turn to the operator $\mathcal{M}$. For our application, we assume that $\mathcal{M} : v \mapsto Mv$ where M is a 4×4 diagonal matrix with diagonal $[m_1\, m_1\, m_1\, m_2]$. To determine the parameters m_1 and m_2 we note that the energy of the bilinear form is

$$a(\boldsymbol{U}, \boldsymbol{U}) = (\mathcal{M}\mathcal{L}^*\boldsymbol{U}, \mathcal{L}^*\boldsymbol{U}) \tag{2.19}$$

$$= (\boldsymbol{B}, \mathcal{M}^{-1}\boldsymbol{B}) \tag{2.20}$$

$$= (m_1^{-1}B, B) + (m_2^{-1}b, b). \tag{2.21}$$

For the exact solution $b = 0$, and we should preferably obtain proportionality to the physical energy

$$\frac{1}{2}(B, H) = \frac{1}{2}(B, \mu^{-1}B), \tag{2.22}$$

and thus $m_1 = \mu$. Next to determine m_2 we note that

$$a(\boldsymbol{U}, \boldsymbol{U}) = (\mu(\mu^{-1}\nabla \times U - \nabla u), (\mu^{-1}\nabla \times U - \nabla u)) + (m_2 \nabla \cdot U, \nabla \cdot U). \tag{2.23}$$

Balancing the terms involving U we are led to choosing $m_2 = \mu^{-1}$.

Using Lemma 2.1 below, the bilinear form finally simplifies to

$$a(\boldsymbol{U}, \boldsymbol{U}) = (\mu^{-1}\nabla \times U, \nabla \times U) + (\mu^{-1}\nabla \cdot U, \nabla \cdot U) + (\mu \nabla u, \nabla u). \tag{2.24}$$

Lemma 2.1. *For $\boldsymbol{V} \in \mathcal{D}(\mathcal{L}^*)$,*

$$(\nabla \times V, \nabla v) = 0. \tag{2.25}$$

Proof. The identity follows using Green's formula,

$$(\nabla \times V, \nabla v) = (V, \nabla \times \nabla v) + (n \times V, \nabla v)_\Gamma, \tag{2.26}$$

since $n \times V = 0$ on $\partial\Omega$ for $\boldsymbol{V} \in \mathcal{D}(\mathcal{L}^*)$. □

We are now ready to state the following theorems.

Theorem 2.1. *There are constants c and C, which depend only on μ, such that*

$$c\|\boldsymbol{V}\|_1^2 \leq a(\boldsymbol{V}, \boldsymbol{V}) \leq C\|\boldsymbol{V}\|_1^2, \tag{2.27}$$

for all $\boldsymbol{V} \in \mathcal{V}$. Furthermore, there exists a unique solution $\boldsymbol{U}$ to (2.16) and the a priori estimate

$$\|\boldsymbol{U}\|_1 \leq c\|\boldsymbol{J}\|_{-1}, \tag{2.28}$$

holds.

Proof. To prove the lower bound we note that

$$a(\boldsymbol{V}, \boldsymbol{V}) = (\mu^{-1}\nabla \times V, \nabla \times V) + (\mu^{-1}\nabla \cdot V, \nabla \cdot V) + (\mu \nabla v, \nabla v)$$

$$\geq \min(\mu^{-1})\|V\|_1^2 + \min(\mu)\|v\|_1^2, \tag{2.29}$$

which concludes the proof of the coercivity. The upper bound is an obvious consequence of the Cauchy-Schwarz and triangle inequalities. The existence and uniqueness of the solution

to (2.16) follows from the Lax-Milgram Lemma and the a priori estimate is straightforward. □

Theorem 2.2. *There is a unique solution $\boldsymbol{B} \in \mathcal{D}(\mathcal{L})$ to (2.4), and $\boldsymbol{B} = \mathcal{M}\mathcal{L}^*\boldsymbol{U}$ is the unique solution to (2.14).*

Proof. First, note that $\mathcal{L}^{-*}$ is continuous, since from Theorem 2.1 we have

$$c\|\boldsymbol{V}\|^2_{\mathcal{D}(\mathcal{L}^*)} \leq \|\mathcal{L}^*\boldsymbol{V}\|^2_{\mathcal{V}}, \tag{2.30}$$

for all $\boldsymbol{V} \in \mathcal{D}(\mathcal{L}^*)$. Choosing $\boldsymbol{V} = \mathcal{L}^{-*}\boldsymbol{W}$ for $\boldsymbol{W} \in \mathcal{R}(\mathcal{L}^*)$, where $\mathcal{R}$ denotes the range, yields,

$$\|\mathcal{L}^{-*}\boldsymbol{W}\|^2_{\mathcal{V}} \leq \frac{1}{c}\|\boldsymbol{W}\|^2_{\mathcal{D}(\mathcal{L}^*)}. \tag{2.31}$$

In the same way, we get continuity of $\mathcal{L}^{-1}$ if we can show

$$\|\boldsymbol{V}\|^2_{\mathcal{D}(\mathcal{L})} \leq C\|\mathcal{L}\boldsymbol{V}\|^2_{\mathcal{V}}, \tag{2.32}$$

which is clear since for $\boldsymbol{V} \in \mathcal{D}(\mathcal{L}^*)$,

$$\begin{aligned} \|\mathcal{L}\boldsymbol{V}\|^2_{\mathcal{V}} &= (\nabla \times \mu^{-1}, \nabla \times \mu^{-1}) + (\nabla v, \nabla v) + (\nabla \cdot V, \nabla \cdot V) \\ &\geq C(\|V\|^2 + \|v\|^2) = C\|\boldsymbol{V}\|^2_{\mathcal{V}}. \end{aligned} \tag{2.33}$$

From Lemma 2.2 in [11], we now know that $\mathcal{R}(\mathcal{L}) = \mathcal{R}(\mathcal{L}^*) = \mathcal{V}$, thus $\boldsymbol{B} = \mathcal{M}\mathcal{L}^*\boldsymbol{U}$ satisfies (2.14). The uniqueness of this solution follows from the stability estimate

$$(\boldsymbol{B}, \mathcal{L}^*) = (\boldsymbol{J}, \boldsymbol{V}) \leq \|\boldsymbol{J}\|\|\boldsymbol{V}\|. \tag{2.34}$$

□

3. The $\mathcal{L}\mathcal{L}^*$ finite element method

3.1. **The finite element method.** Let $\mathcal{K}$ be a decomposition of Ω into, e.g., tetrahedral, elements K, with diameter $h_K = \text{diam}(K)$. We assume a minimal angle condition on the triangulation, see Brenner and Scott [8]. Let

$$\mathcal{W}_h = \mathcal{D}(\mathcal{L}^*) \cap \{\boldsymbol{V} \in [C(\Omega)]^4 : \boldsymbol{V}|_K \in [\mathcal{P}_r(K)]^4\}, \tag{3.1}$$

where $\mathcal{P}_r$ is the vector space of all polynomials of degree less than or equal to r. Thus $\mathcal{W}_h$ is the set of all piecewise vector polynomial functions of degree r, which are continuous in the subdomains Ω^i such that, in each element, $v|_K \in \mathcal{P}_r(K)$.

For the error analysis following below, we need the following approximation property of $\mathcal{W}_h$, see Scott and Zhang [16]. Given a function $\boldsymbol{V} \in \mathcal{D}(\mathcal{L}^*) \cap [H^\alpha(\Omega)]^4$, for $r \geq 1$, there is an interpolation operator $\pi : \mathcal{D}(\mathcal{L}^*) \to \mathcal{W}_h$ such that

$$\|\boldsymbol{V} - \pi\boldsymbol{V}\|_{K,1} \leq Ch_K^{\alpha-1}|\boldsymbol{V}|_{N(K),r+1}, \quad 1 \leq \alpha \leq r+1, \tag{3.2}$$

where $N(K)$ denotes the union of all elements bordering K.

The $\mathcal{LL}^*$ finite element method finally takes the form: find $\boldsymbol{U}_h \in \mathcal{W}_h$ such that

$$a(\boldsymbol{U}_h, \boldsymbol{V}) = l(\boldsymbol{V}), \tag{3.3}$$

for all $\boldsymbol{V} \in \mathcal{W}_h$.

In the computations, we can benefit from the fact that u_h is zero. This is clear since the equations for components U_h and u_h separates according to Lemma 2.1, and we have zero data for u_h. The bilinear form and functional used in computations thus takes the form

$$a_h(\boldsymbol{U}, \boldsymbol{V}) = (\mu^{-1}\nabla \times U, \nabla \times V) + (\mu^{-1}\nabla \cdot U, \nabla \cdot V), \tag{3.4a}$$

$$l_h(\boldsymbol{V}) = (J, V). \tag{3.4b}$$

Furthermore, functionals involving the magnetic field B, should be computed via the variational form (3.4a). Hence the energy, e.g., is computed as

$$W_h = \frac{1}{2} a_h(\boldsymbol{U}_h, \boldsymbol{U}_h). \tag{3.5}$$

3.2. **A priori error estimate.** Using standard techniques we derive the following a priori error estimate.

Theorem 3.1. *Let $\boldsymbol{U} \in \mathcal{D}(\mathcal{L}^*) \cap H^s(\Omega)$ be a solution to (2.16) and $\boldsymbol{U}_h \in \mathcal{W}_h$ the approximate solution defined by (3.3). Then there is a constant C, independent of h, such that*

$$\|\boldsymbol{U} - \boldsymbol{U}_h\|_1^2 \leq C \sum_{K \in \mathcal{K}} h_K^{2(\alpha-1)} |\boldsymbol{U}|_{N(K),\alpha}^2, \tag{3.6}$$

with $\alpha = \max(r+1, s)$.

Proof. Let $\boldsymbol{E} = \boldsymbol{U} - \boldsymbol{U}_h$ denote the error. Then

$$\begin{aligned} c\|\boldsymbol{E}\|_1^2 &\leq a(\boldsymbol{E}, \boldsymbol{U} - \boldsymbol{U}_h) \\ &= a(\boldsymbol{E}, \boldsymbol{U} - \pi\boldsymbol{U} + \pi\boldsymbol{U} - \boldsymbol{U}_h) \\ &= a(\boldsymbol{E}, \boldsymbol{U} - \pi\boldsymbol{U}) \\ &\leq C\|\boldsymbol{E}\|_1^2 \|\boldsymbol{U} - \pi\boldsymbol{U}\|_1^2, \end{aligned} \tag{3.7}$$

where (3.3) was used in the last equality. Dividing by $\|\boldsymbol{E}\|_1$, and finally using the interpolation estimate (3.2) proves the estimate. □

3.3. **A posteriori error estimate.** Introducing the energy norm

$$|||v|||^2 = a(v, v), \tag{3.8}$$

we can state the following energy norm a posteriori error estimate.

Theorem 3.2. *Let $\boldsymbol{U} \in \mathcal{D}(\mathcal{L}^*) \cap H^1(\Omega)$ be a solution to (2.16) and $\boldsymbol{U}_h \in \mathcal{W}_h$ the approximate solution defined by (3.3). Then there is a constant C, independent of h, such that*

$$|||\boldsymbol{U} - \boldsymbol{U}_h|||^2 \leq C \sum_{K \in \mathcal{K}} R_K(\boldsymbol{U}_h)^2, \tag{3.9}$$

where

$$R_K(\boldsymbol{U}_h)^2 = \omega_1 \|h\mathcal{M}^{-1/2}(\boldsymbol{J} - \mathcal{L}\mathcal{M}\mathcal{L}^*\boldsymbol{U}_h)\|_K^2 + \omega_2 \|h^{1/2} K[\lambda_n(\boldsymbol{U}_h)]\|_{\partial K}^2. \tag{3.10}$$

The boundary flux $\lambda_n(\boldsymbol{V})$ is defined by

$$\lambda_n(\boldsymbol{V}) = \begin{pmatrix} n \times (\mu^{-1}\nabla \times V) + n\mu^{-1}\nabla \cdot V \\ n \cdot (\mu \nabla v) \end{pmatrix}, \tag{3.11}$$

and K is a diagonal matrix with diagonal $[k_1 k_1 k_1 k_2]$ where

$$k_1 = \frac{(\mu^+)^{1/2}}{\mu^+ + \mu^-}, \tag{3.12a}$$

$$k_2 = \frac{(\frac{1}{\mu^+})^{1/2}}{\frac{1}{\mu^+} + \frac{1}{\mu^-}}. \tag{3.12b}$$

Remark 3.1 Note that the constant $C = C(\omega_1, \omega_2, C_{tr}, C_i)$. To achieve a constant free error estimator, one may instead solve local problems, see [2], in general at the cost of more expensive computations.

Remark 3.2 Note that

$$|||\boldsymbol{U} - \boldsymbol{U}_h||| = a(\boldsymbol{U} - \boldsymbol{U}_h, \boldsymbol{U} - \boldsymbol{U}_h) = a(\boldsymbol{U}, \boldsymbol{U}) - a(\boldsymbol{U}_h, \boldsymbol{U}_h) = 2(W - W_h). \tag{3.13}$$

Thus the error in the energy is directly related to the error in the energy norm, motivating adaptation of the grid with respect to the error measured in the energy norm.

Proof. Let $\boldsymbol{E} = \boldsymbol{U} - \boldsymbol{U}_h$ denote the error. Then

$$\begin{aligned} |||\boldsymbol{E}|||^2 &= a(\boldsymbol{U} - \boldsymbol{U}_h, \boldsymbol{E}) \\ &= a(\boldsymbol{U} - \boldsymbol{U}_h, \boldsymbol{E} - \pi\boldsymbol{E}) \\ &= (\mathcal{M}\mathcal{L}^*(\boldsymbol{U} - \boldsymbol{U}_h), \mathcal{L}(\boldsymbol{E} - \pi\boldsymbol{E})) \\ &= \sum_{K \in \mathcal{K}} (\boldsymbol{J} - \mathcal{L}\mathcal{M}\mathcal{L}^*\boldsymbol{U}_h, \boldsymbol{E} - \pi\boldsymbol{E})_K + (\lambda_n(\boldsymbol{U}) - \lambda_n(\boldsymbol{U}_h), \boldsymbol{E} - \pi\boldsymbol{E})_{\partial K} \\ &= \sum_{K \in \mathcal{K}} (\boldsymbol{J} - \mathcal{L}\mathcal{M}\mathcal{L}^*\boldsymbol{U}_h, \boldsymbol{E} - \pi\boldsymbol{E})_K + (\Lambda_n(\boldsymbol{U}_h) - \lambda_n(\boldsymbol{U}_h), \boldsymbol{E} - \pi\boldsymbol{E})_{\partial K}, \end{aligned} \tag{3.14}$$

where $\lambda_n(\boldsymbol{V})$ is defined above in (3.11) and $\Lambda_n(\boldsymbol{U}_h)$ is a discrete approximation of the true flux $\lambda_n(\boldsymbol{U})$. The replacement of $\lambda_n(\boldsymbol{U})$ with $\Lambda_n(\boldsymbol{U}_h)$ in the last equality is possible since on all internal edges the boundary contributions from the neighbouring elements cancel for

$\lambda_n(\boldsymbol{U})$, and this should be true for $\Lambda_n(\boldsymbol{U}_h)$ by construction, as well as on external edges $\Lambda_n(\boldsymbol{U}_h)$ should satisfies the boundary conditions.

In a standard derivation of an energy norm a posteriori error estimate,e.g., as in Eriksson and Johnson [12], one constructs a discrete flux as the average of the approximate flux on each element side, i.e.

$$\Lambda_n(\boldsymbol{U}_h) = \frac{1}{2}(\lambda_n(\boldsymbol{U}_h^+) + \lambda_n(\boldsymbol{U}_h^-)), \tag{3.15}$$

which leads to the standard jump terms $\frac{1}{2}[\lambda_n(\boldsymbol{U}_h)]$. However, in order to correctly distribute the error in the fluxes across interfaces with large discontinuities in μ, we here choose a weighted average

$$\Lambda_n(\boldsymbol{U}_h) = (M^+ + M^-)^{-1}(M^-\lambda_n(\boldsymbol{U}_h^+) + M^+\lambda_n(\boldsymbol{U}_h^-)), \tag{3.16}$$

which instead lead to a jump term similar to the one derived by Cai and Samuelsson [9].

We will now get

$$\begin{aligned}
|||\boldsymbol{E}|||^2 &= \sum_{K\in\mathcal{K}} (\boldsymbol{J} - \mathcal{L}\mathcal{M}\mathcal{L}^*\boldsymbol{U}_h, \boldsymbol{E} - \pi\boldsymbol{E})_K \\
&\quad + (\Lambda_n(\boldsymbol{U}_h) - \lambda_n(\boldsymbol{U}_h), \boldsymbol{E} - \pi\boldsymbol{E})_{\partial K} \\
&= \sum_{K\in\mathcal{K}} (\boldsymbol{J} - \mathcal{L}\mathcal{M}\mathcal{L}^*\boldsymbol{U}_h, \boldsymbol{E} - \pi\boldsymbol{E})_K \\
&\quad + ((M^+ + M^-)^{-1}M^+[\lambda_n(\boldsymbol{U}_h)], \boldsymbol{E} - \pi\boldsymbol{E})_{\partial K} \\
&\le C \sum_{K\in\mathcal{K}} (\|h\mathcal{M}^{-1/2}(\boldsymbol{J} - \mathcal{L}\mathcal{M}\mathcal{L}^*\boldsymbol{U}_h)\|_K \|h^{-1}\mathcal{M}^{1/2}(\boldsymbol{E} - \pi\boldsymbol{E})\|_K \\
&\quad + \|h^{1/2}(M^+ + M^-)^{-1}(M^+)^{1/2}[\lambda_n(\boldsymbol{U}_h)]\|_{\partial K} \|h^{-1/2}M^{1/2}(\boldsymbol{E} - \pi\boldsymbol{E})\|_{\partial K}) \\
&\le C \left(\sum_{K\in\mathcal{K}} R(\boldsymbol{U}_h)^2 \right)^{1/2} |||\boldsymbol{E}|||,
\end{aligned} \tag{3.17}$$

where we made use of the Cauchy-Schwarz inequality and the trace inequality $\|v\|_{\partial K}^2 \le C\|v\|_K(h_K^{-1}\|v\|_K + \|\nabla v\|_K)$. Finally the aforementioned approximation property

$$\|h^{-1}\mathcal{M}^{1/2}(\boldsymbol{V} - \pi\boldsymbol{V})\|^2 \le C|\mathcal{M}^{1/2}\boldsymbol{V}|_1^2 \le C\|\mathcal{M}^{1/2}\nabla\boldsymbol{V}\|^2 \le C|||V|||^2$$

was used. □

3.4. **An adaptive algorithm.** We start the adaptive algorithm from an initial coarse decomposition $\mathcal{K}_0$ consisting of tetrahedra. It is important that the interfaces between discontinuous materials are respected by the triangulation, i.e., the material interfaces consist of element sides.

The initial triangulation is then adaptively refined level by level. There are two main components in this process: the error estimator and the local grid refiner. The role of the error estimator is to locally determine which elements are to be bisected to construct a

refined grid. It is not critical which refinement method is used, except that it should have the property that the refinement is stable, i.e., the refined grid should remain shape regular even after many adaptive local refinements.

We will briefly describe the refinement method used in our implementation. The refinement algorithm is also used in [9] and implemented in the adaptive module of [1].

- Compute for each element K of the triangulation an indicator value I_K, where a large value of I_K indicates a large error. Based on the a posteriori estimate (3.9) we use $I_K = R_K(\boldsymbol{U}_h)^2$.
- From the indicator values I_K , each tetrahedron K of $\mathcal{K}$ is assigned an integer $i_K \in \{0, 1, 2, 3, 4, 5, 6\}$. The integer i_K denotes the minimal number of edges of tetrahedron K where new nodes are inserted in the refinement.

  Given a parameter $\beta \in (0, 1)$ and the maximal indicator value $I_{max} = \max_{K\in\mathcal{K}} I_K$ the integer i_K is computed by

$$i_K = \begin{cases} 0 & \text{if} \quad I_K \leq \beta^6 I_{max}, \\ j & \text{if} \quad \beta^{7-j} I_{max} < I_K \leq \beta^{6-j} I_{max} \quad \text{for} \quad j = 1, \ldots 6. \end{cases}$$

- Mark the i_K longest edges in the elements for new node insertion. By the next step the neighbour elements might need to mark additional edges to guarantee stability of the refinement.
- The following two rules are recursively applied to mark the neighbour elements: If any edge in a tetrahedron is marked, then the longest edge is also marked, and if any edge on a face of a tetrahedron is marked, then the longest edge of that face is also marked.
- The tetrahedra having any marked edges is refined by repeated bisection until there are no more marked edges. The length of the marked edges of the tetrahedron determines the order of tetrahedral bisection. The longest edge is bisected first which together with the marking of edges in the previous step guarantees that the refinement will be regular.
- Project nodes at the curved outer boundaries or internal interfaces to the correct geometry.

The method have the property that the sequence of grid refinements are nested and the minimum number of edges where new nodes are added to the refined grid is controlled. If the geometry model has curved outer boundaries or internal interfaces the refinement will not be strictly nested, due to that the newly introduced nodes need to conform to the curved geometry model. For more information on the geometry model and implementational issues we refer to [4].

4. The multigrid method

Let $\mathcal{K}_k, k = 0, \ldots, m$ be a sequence of decompositions of Ω and let $\mathcal{W}_{h,k}, k = 0, \ldots, m$, be the associated spaces of piecewise vector polynomial functions. We assume that the spaces are nested $\mathcal{W}_{h,0} \subset \mathcal{W}_{h,1} \subset \ldots \subset \mathcal{W}_{h,m}$.

The operator $A_k : \mathcal{W}_{h,k} \mapsto \mathcal{W}_{h,k}$ is defined by $(A_k \boldsymbol{U}_k, \boldsymbol{V}) = a(\boldsymbol{U}_k, \boldsymbol{V})$ for all $\boldsymbol{V} \in \mathcal{W}_{h,k}$ and L_k by $L_k \boldsymbol{V} = l(\boldsymbol{V})$ for all $\boldsymbol{V} \in \mathcal{W}_{h,k}$. The finite element discretization (3.3) on $\mathcal{K}_k$ then takes the form

$$A_k \boldsymbol{U}_k = L_k,$$

for $k = 0, \ldots, m$.

We define the projection operator $Q_k : \mathcal{W}_{h,k+1} \mapsto \mathcal{W}_{h,k}$ by

$$(Q_k \boldsymbol{U}, \boldsymbol{V}) = (\boldsymbol{U}, \boldsymbol{V}) \quad \text{for all } \boldsymbol{V} \in \mathcal{W}_{h,k}.$$

We denote one multigrid V-cycle with (n_1, n_2) pre- and post-smoothing operations by $T = T_k$ where $T_k : \mathcal{W}_{h,k} \mapsto \mathcal{W}_{h,k}$, $1 \le k \le m$, is defined recursively by $T_0 = A_0^{-1}$ and

$$T_k L = v^{n_1+n_2+1},$$

where

$$\begin{aligned}
v^0 &= \begin{cases} 0 & \text{if} \quad k < m \\ \boldsymbol{U}_{m-1} & \text{if} \quad k = m \end{cases} \\
v^j &= v^{j-1} + S_k(L - A_k v^{j-1}), \quad \text{for } j = 1, \ldots, n_1, \\
v^{n_1+1} &= T_{k-1} Q_{k-1}(L - A_k v^{n_1}), \\
v^j &= v^{j-1} + S_k(L - A_k v^{j-1}), \quad \text{for } j = n_1 + 2, \ldots, n_1 + n_2 + 1.
\end{aligned}$$

Here $S_k : \mathcal{W}_{h,k} \mapsto \mathcal{W}_{h,k}$ represents one smoothing operation which can consist of a step of a preconditioned Krylov method.

5. Examples

The $\mathcal{LL}^*$ method described above was tested for problem (2.1) in three dimensions on an axisymmetric geometry that describes an electromagnet, see Figures 2 and 3. The model consists of an iron cylinder core inserted in a copper winding. The configuration is enclosed in air and surrounded by a box with perfectly conducting surfaces. The winding is modeled as a homogeneous copper coil.

Data for the problem are relative magnetic permeabilities of $\mu_{r,Fe} = 10^4$ and $\mu_{r,Cu} = \mu_{r,air} = 1$ and $\mu_0 = 4\pi \times 10^{-7}$ H/m and a current density J that is constant over the cross section of the coil with a total current of 1 A.

The geometry and data for the test problem was suggested by ABB Corporate Research, who also provided reference two dimensionally axisymmetric solutions, reported in [4]. Note that the problem includes a large discontinuity in the coefficients of the problem, as well as edges where the field solution is singular.

The problem was solved using multigrid as described above, with three iterations of GMRES, preconditioned with one SSOR sweep at each level. The coarsest problem was solved using stabilized bi-conjugated gradient (BCGSTAB). Mesh adaptation was based on the energy norm a posteriori error indicator derived above.

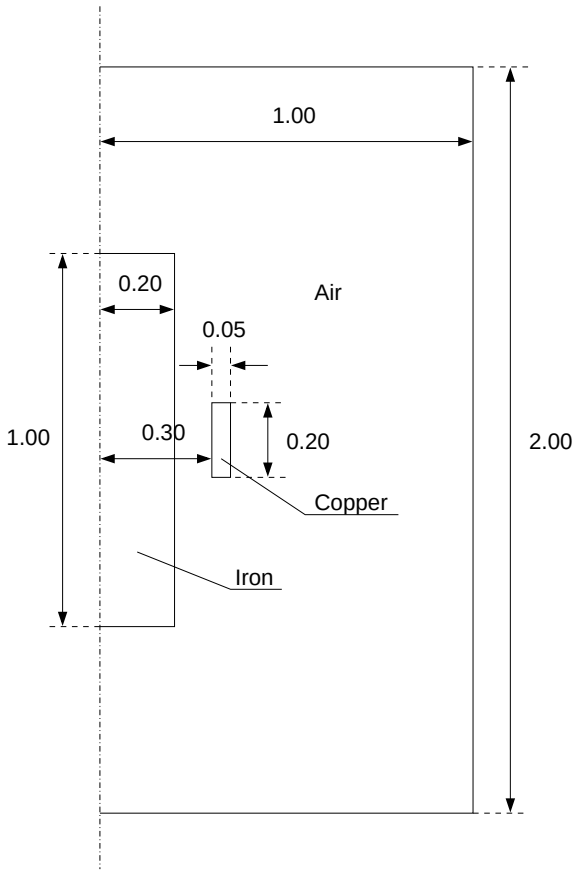

FIGURE 2. The geometry of the axisymmetric problem. The dimensions are given in meters.

Table 1 gives the errors in energy, ϵ_r, and the solution times, t_s, on each level of the computation. The error is defined as

$$\epsilon_r = \frac{\|W_{ref} - W_h\|}{\|W_{ref}\|}, \tag{5.1}$$

where W_{ref} denotes the magnetic energies in the reference solution computed by ABB, and W_h denotes the ones computed from the $\mathcal{LL}^*$ solutions through (3.5). The actual computed energies are shown in Table 2 for the finest mesh.

Due to the use of unstructured grids together with non-uniform mesh refinement, asymptotic order of convergence is difficult to measure. However, in Figure 4 we show convergence of the error in energy compared with the error indicator, and we can see that the error shows the same behaviour as the indicator. Thus, the convergence rate appears to be $O(h)$ as expected.

The convergence in multigrid is measured by the decrease in algebraic residual between two V-cycles on the same level in the grid hierarchy. In Table 3 these factors, called ρ,

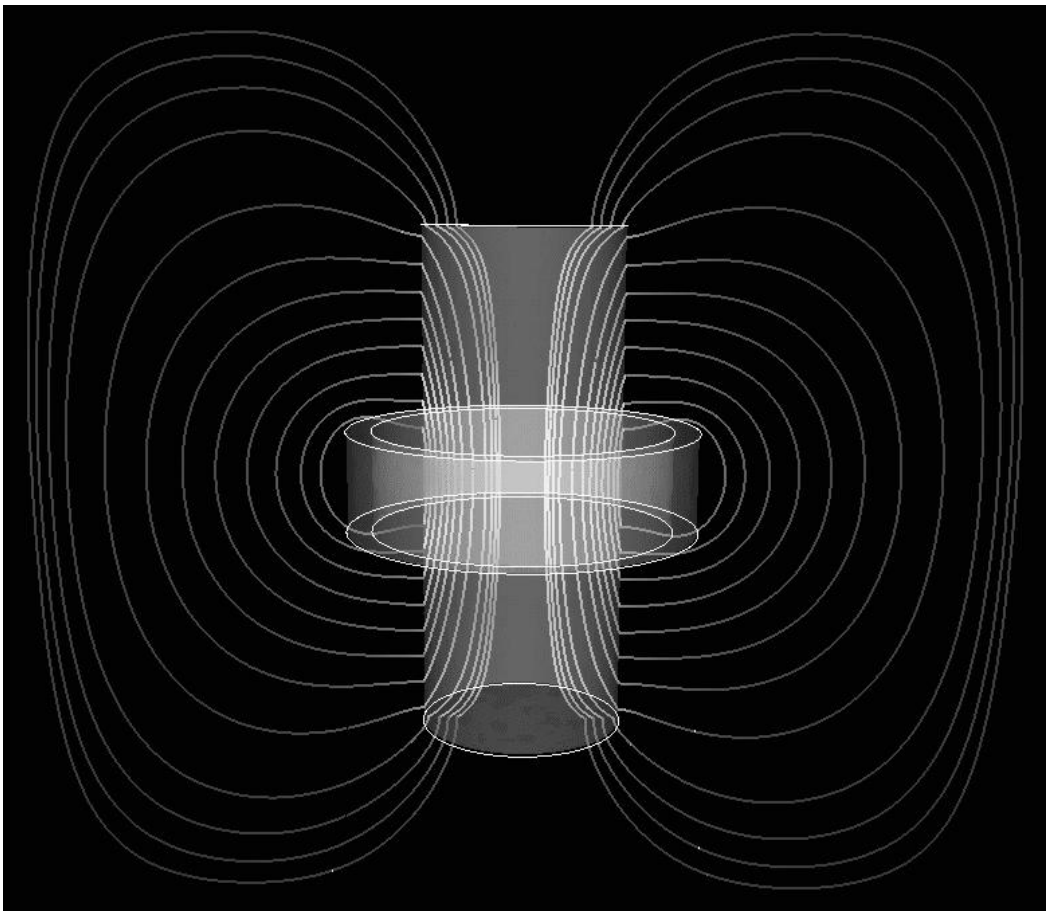

FIGURE 3. The magnetic field lines in a slice through the three dimensional solution of the axisymmetric problem.

$\text{No}_{elements}$	No_{nodes}	t_s [s]	$\epsilon_{r,air}$	$\epsilon_{r,Fe}$	$\epsilon_{r,Cu}$	$\epsilon_{r,total}$
14401	2580	4.1	0.23	0.47	0.47	0.24
32498	5938	41.29	0.14	0.33	0.29	0.15
104304	18868	172.56	0.07	0.18	0.13	0.07
294521	53417	967.69	0.04	0.09	0.07	0.04
645947	116506	3257.73	0.02	0.05	0.05	0.02
970767	175165	6331.57	0.02	0.04	0.03	0.02

TABLE 1. The time to solve the problem on each level and relative error in the computed magnetic energies using $\mathcal{LL}^*$ and piecewise linear polynomial elements. The reference values are from two dimensional computations done at ABB, see [4].

	Linear	Reference
W_{air} (J)	8.947e-7	9.089e-7
W_{Fe} (J)	4.539e-10	4.731e-10
W_{Cu} (J)	3.494e-8	3.614e-8
W_{total} (J)	9.301e-7	9.455e-7

TABLE 2. The computed magnetic energies compared with reference values using $\mathcal{LL}^*$ and piecewise linear polynomial elements. The mesh used to obtain these values had 970,767 elements and 175,165 nodes. The reference values are from two dimensional computations done at ABB, see [4].

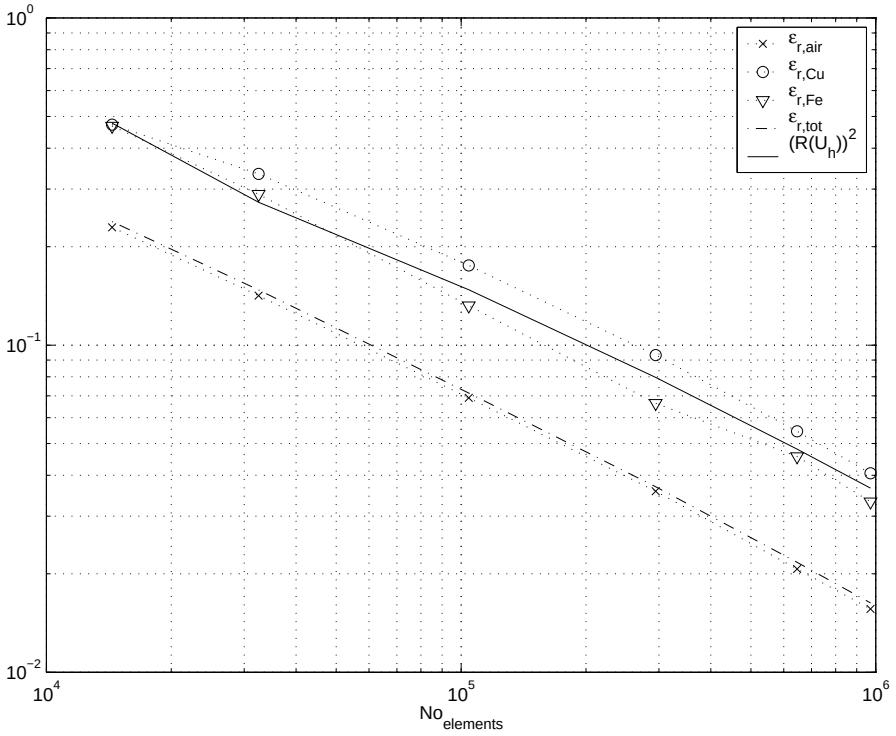

FIGURE 4. Convergence in error compared with the indicator derived in Section 3.3.

are given as the geometric mean value for all V-cycles on each level, and for different sizes of the discontinuity in material parameters. As expected, the convergence increases for smaller discontinuities.

Acknowledgements. This research is supported by ABB Corporate Research, Sweden, and the Swedish Foundation for Strategic Research.

$\frac{\mu_{Fe}}{\mu_{air}}$	$\mathrm{No}_{elements}$	No_{nodes}	ρ
10000	14401	2580	2.43e-14
	32498	5938	1.42e-1
	104304	18868	3.59e-1
	294521	53417	6.13e-1
	645947	116506	7.21e-1
	970767	175165	7.07e-1
1000	14401	2580	2.36e-14
	32282	5898	9.86e-2
	104162	18850	2.87e-1
	294581	53430	4.92e-1
	582500	105255	5.86e-1
	1318174	237107	6.67e-1
100	14401	2580	2.26e-14
	31418	5741	4.90e-2
	102341	18515	1.65e-1
	266466	48356	2.33e-1
	594002	107212	2.89e-1
	1235205	222242	2.94e-1
10	14401	2580	1.66e-14
	25239	4583	9.74e-3
	84852	15395	2.86e-2
	193051	34983	3.25e-2
	492963	89041	3.38e-2
	1098954	197763	3.38e-2
1	14401	2580	7.66e-15
	21895	3982	6.69e-3
	55870	10095	8.64e-3
	96370	17475	9.53e-3
	290141	52226	1.18e-2
	516202	93285	1.03e-2

TABLE 3. Convergence factors for the multigrid iterations for different sizes of discontinuity. The factor ρ is the geometric mean of the decrease in the algebraic residual between two consecutive V-cycles for all V-cycles on each level.

References

[1] Diffpack home page. http://www.nobjects.com/Products/Diffpack.

[2] R.E. Banks and A. Weiser. Some a posteriori error estimators for elliptic partial differential equations. *Math. Comp.*, (44):283–301, 1985.

[3] R. Bergström. Least-squares finite element methods for electromagnetic applications. Preprint 5, Chalmers Finite Element Center, Chalmers University of Technology, 2000.

[4] R. Bergström, A. Bondeson, C. Johnson, M.G. Larson, Y. Liu, and K. Samuelsson. Adaptive finite element methods in electromagnetics. Technical Report 2, Swedish Institute of Applied Mathematics (ITM), 1999.

[5] M. Berndt, T.A. Manteuffel, and S.F. McCormick. Local error estimates and adaptive refinement for first-order system least squares (FOSLS). *Electron. Trans. Numer. Anal.*, pages 35–43, Dec 1997.

[6] P.B. Bochev and M.D. Gunzburger. Finite element methods of least-squares type. *SIAM Rev.*, 40(4):789–837, 1998.

[7] J.H. Bramble, R.D. Lazarov, and J.E. Pasciak. A least-squares approach based on a discrete minus one inner product for first order systems. *Math. Comp.*, 66:935–955, 1997.

[8] S.C. Brenner and L.R. Scott. *The Mathematical Theory of Finite Element Methods.* Springer-Verlag, 1994.

[9] X. Cai and K. Samuelsson. Parallel multilevel methods with adptivity on unstructerd grids. *Comput. Visual Sci.*, 3:133–146, 2000.

[10] Z. Cai, A. Mantueffel, S. McCormick, and S. Parter. First-order system least squares for planar linear elasticity: pure traction. *SIAM J. Numer. Anal.*, (35):320–335, 1998.

[11] Z. Cai, A. Mantueffel, S. McCormick, and J. Ruge. First-order system $\mathcal{LL}^*$ (FOSLL*):scalar elliptic partial differential equations. submitted, 2000.

[12] K. Eriksson and C. Johnson. Adaptive finite element methods for prabolic problems I: A linear model problem. *SIAM J. Numer. Anal*, 28:43–77, 1991.

[13] B.-N. Jiang. *Least-squares finite element method : Theory and applications in computational fluid dynamics and electromagnetics.* Springer-Verlag, 1998.

[14] B.-N. Jiang, J. Wu, and L.A. Povinelli. The origin of spurious solutions in computational electromagnetics. *J. Comp. Phys.*, 125:104–123, 1996.

[15] J. Jin. *The Finite Element Method in Electromagnetics.* John Wiley & Sons, Inc., 1993.

[16] L.R. Scott and S. Zhang. Finite element interpolation of nonsmooth functions satisfying bundary conditions. *Math. Comp.*, 54:483–493, 1990.

Chalmers Finite Element Center Preprints

2000–01 *Adaptive Finite Element Methods for the Unsteady Maxwell's Equations*
Johan Hoffman

2000–02 *A Multi-Adaptive ODE-Solver*
Anders Logg

2000–03 *Multi-Adaptive Error Control for ODEs*
Anders Logg

2000–04 *Dynamic Computational Subgrid Modeling* (Licentiate Thesis)
Johan Hoffman

2000–05 *Least-Squares Finite Element Methods for Electromagnetic Applications* (Licentiate Thesis)
Rickard Bergström

2000–06 *Discontinuous Galerkin methods for incompressible and nearly incompressible elasticity by Nitsche's method*
Peter Hansbo and Mats G. Larson

2000–07 *A Discountinuous Galerkin Method for the Plate Equation*
Peter Hansbo and Mats G. Larson

2000–08 *Conservation Properties for the Continuous and Discontinuous Galerkin Methods*
Mats G. Larson and A. Jonas Niklasson

2000–09 *Discontinuous Galerkin and the Crouzeix-Raviart element: Application to elasticity*
Peter Hansbo and Mats G. Larson

2000–10 *Pointwise A Posteriori Error Analysis for an Adaptive Penalty Finite Element Method for the Obstacle Problem*
D A French, S Larson and R H Nochetto

2000–11 *Global and Localised A Posteriori Error Analysis in the maximum norm for finite element approximations of a convection-diffusion problem*
Mats Boman

2000–12 *A Posteriori Error Analysis in the maximum norm for a penalty finite element method for the time-dependent obstacle problem*
Mats Boman

2000–13 *A Posteriori Error Analysis in the maximum norm for finite element approximations of a time-dependent convection-diffusion problem*
Mats Boman

2001–01 *A Simple Nonconforming Bilinear Element for the Elasticity Problem*
Peter Hansbo and Mats G. Larson

2001–02 *The $\mathcal{LL}^*$ Finite Element Method and Multigrid for the Magnetostatic Problem*
Rickard Bergström, Mats G. Larson, and Klas Samuelsson

These preprints can be obtained from

`www.phi.chalmers.se/preprints`